

Brillouin light scattering from pumped uniform-precession and low- k magnons in $\text{Ni}_{81}\text{Fe}_{19}$

Ward L. Johnson,^{a)} Sudook A. Kim, Stephen E. Russek, and Pavel Kabos
National Institute of Standards and Technology, 325 Broadway, Boulder, Colorado 80305

(Received 13 September 2004; accepted 4 February 2005; published online 4 March 2005)

A method is presented for performing Brillouin-light-scattering measurements on uniform-precession and low-wave-number (low- k) magnons excited by a microwave magnetic field in opaque magnetic specimens. The optical configuration is similar to that employed in conventional 180° backscattering measurements, except that the incident and specularly reflected beams pass through the collection lens along different parallel paths. Examples of spectra from a $\text{Ni}_{81}\text{Fe}_{19}$ film are presented that include separate detection of light scattered from low- k magnons with the same frequency as the uniform precession. [DOI: 10.1063/1.1882754]

Information on externally excited low-wave-number (low- k) magnetic excitations in thin magnetic films has been of increasing interest in recent years, partly in relation to soliton propagation and interaction^{1,2} and applications that employ impulse techniques.^{3–5} Brillouin light scattering (BLS) can provide information on the dispersion relations of magnons but has been used only rarely with microwave excitation in metallic films. This is because the traditional approach for detecting uniform-precession or low- k magnons has been in a forward-scattering configuration, which can be employed only on specimens that transmit a significant fraction of the incident light. For example, Srinivasan, Patton, and Booth⁶ demonstrated that forward scattering from pumped uniform-precession magnons could be detected in films of $\text{Ni}_{81}\text{Fe}_{19}$ (Permalloy) with a thickness of 22–75 nm.

To overcome the limitations of the forward-scattering configuration, Wettling and Jantz⁷ pioneered a backscattering approach to BLS measurements of pumped uniform-precession magnons. They used this technique to study ferromagnetic resonance (FMR) in thin Fe films and bulk FeBO_3 but did not present details of the method. Demokritov⁸ developed a hybrid of backscattering and forward-scattering configurations for studying FMR in metallic films, but this approach is relatively difficult to implement. In this letter, we describe a simpler experimental approach that is more easily implemented with a standard BLS system.⁹ As a demonstration of the method, we present spectra including peaks from low- k magnons that are degenerate with the uniform-precession magnons in an electromagnetically excited ferromagnetic film.

The experimental system employs a solid-state diode-pumped frequency-doubled Nd:Vanadate (Nd:YVO_4) laser with a wavelength of 532 nm. The laser is operated at 2 to 3 W to maintain optimal performance. The beam is subsequently attenuated to a level suitable for BLS using a half-wave plate followed by a high-power Glan-Taylor calcite polarizer. The vertically polarized light then passes through a 2 mm diameter collimator and 20 mW is reflected by a 5 mm polarizing beamsplitter cube through an aspherical $f/1.2$ camera (collection) lens with a focal length of 50 mm. The surface of a specimen is located at the focal point and is perpendicular to the axis of the collection lens.

Light that is specularly reflected or scattered from the specimen passes back through the collection lens and through a dichroic sheet polarizer that transmits the horizontal polarization (perpendicular to the light incident on the specimen). Then, the light is focused with an aspherical lens onto a 0.45 mm diameter pinhole that passes light to a standard scanning (3+3)-pass tandem Fabry–Perot interferometer.⁹

The polarizing beamsplitter cube is positioned 3.3 mm off the axis of the collection lens, so that the incident and specularly reflected beams pass along different paths parallel to the axis. This configuration overcomes problems in focusing that we encountered with the cube on-axis. The cube introduces a slight angular shift of light, so that, when it is on the axis, the focal point of light scattered from uniform-precession magnons is displaced in the plane of the pinhole relative to light from low- k magnons that does not pass through the cube. A similar effect was observed with a large pellicle beamsplitter, and this may be associated with heating of the pellicle by the specularly reflected light. The focusing problem might be avoided by using a polarizing beamsplitter cube as large as the aperture of the collection lens, if measurements of only magnetic excitations are of interest, or by using a nonpolarizing beam-splitter cube of similar dimensions, if a 50% reduction in backscattered light is acceptable.

The scattering geometry is shown schematically in Fig. 1 for the case where the backscattered wave vector is in the same plane as the incident and specularly reflected wave vectors. The wave vectors of the incident and reflected light at the surface of the specimen are \mathbf{k}_0 and \mathbf{k}_1 , respectively. The

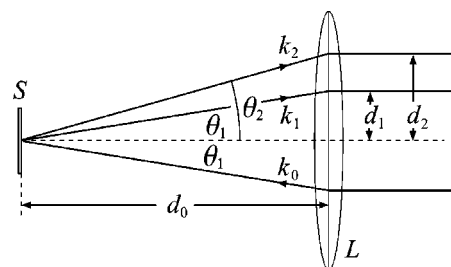


FIG. 1. Wave vectors of light incident (\mathbf{k}_0), specularly reflected (\mathbf{k}_1), and inelastically scattered (\mathbf{k}_2) from a specimen S , which is at the focus of collection lens L .

^{a)}Electronic mail: wjohnson@boulder.nist.gov

incident beam passes through the collection lens at a distance d_1 from the axis, and the specularly reflected beam is offset by the same distance on the other side of the axis. The uncertainty in the perpendicular components of the wave vectors of light in the specimen is inversely proportional to the penetration depth. The selection rule for the parallel components is

$$\pm(\mathbf{q})_{\parallel} = (\mathbf{k}_2)_{\parallel} - (\mathbf{k}_0)_{\parallel} = (\mathbf{k}_2)_{\parallel} - (\mathbf{k}_1)_{\parallel}, \quad (1)$$

where $(\mathbf{q})_{\parallel}$ is the component of the magnon wave vector parallel to the surface of the specimen, and $(\mathbf{k}_0)_{\parallel}$, $(\mathbf{k}_1)_{\parallel}$, $(\mathbf{k}_2)_{\parallel}$ are, respectively, the components of wave vectors parallel to the surface for light that is incident, specularly reflected, and scattered from magnons. For the geometry of Fig. 1, Eq. (1) can be written as

$$(\mathbf{q})_{\parallel} = \pm |\mathbf{k}_0| \left[\frac{d_2}{(d_0^2 + d_2^2)^{1/2}} - \frac{d_1}{(d_0^2 + d_1^2)^{1/2}} \right]. \quad (2)$$

The specimen was mounted on the inside surface of a rectangular TE₁₀₃ X band cavity, covering a 2 mm diameter hole that enabled simultaneous microwave and optical access to the specimen. The cavity was placed between the poles of an electromagnet that supplied a static magnetic field perpendicular to the RF magnetic field. A diode detector with an attenuator was used to monitor the reflected power. The resonant frequency of the cavity was 8.8 GHz, the Q was ~ 1200 , and the reflection coefficient at resonance was at the -16 ± 3 dB level.

The cavity was driven by a traveling-wave-tube (TWT) amplifier with continuous-wave input from an analog signal generator. A feedback loop was used to automatically tune the RF excitation to the resonant frequency of the cavity when the microwave power and/or magnetic field were changed. This was accomplished by modulating the frequency of the source at a rate of 1 kHz around the central frequency. The output from the diode detector was passed to a lock-in amplifier, and the integrated output from the lock-in controlled the offset of the frequency of the signal generator. The magnetic field necessary to bias the magnetic film at FMR was manually adjusted to provide maximum power absorption in the film.

The specimen was a 50 nm film of Ni₈₁Fe₁₉ (Permalloy) sputtered on a glass substrate. Figure 2(a) shows a BLS spectrum with 813 mW of microwave power at 8.8 GHz, and Fig. 2(b) shows a spectrum with no microwave excitation. The ordinates in this figure are the counts per unit time in one channel of the multichannel analyzer. The applied static field at FMR was 67.2 kA/m (845 Oe). The strongly enhanced peaks in Fig. 2(a) at the pumping frequency arise primarily from inelastic light scattering from the uniform-precession magnons excited by the microwave field at FMR. The spectrum shown in Fig. 2(b) arises from inelastic scattering from thermal magnons that are present with the applied static field corresponding to the FMR resonant frequency of 8.8 GHz.

Figure 3 shows the dependence of the count rate (the average of the Stokes and anti-Stokes peaks at ± 8.8 GHz) on the pumping power. The slope of the linear fit in this figure, $(7.0 \pm 0.2) \times 10^3$ counts/J, can be used to estimate the scattering cross section per magnon. Following from the expression for dynamic magnetic energy density presented by Safonov,¹⁰ the number N_u of uniform-precession magnons excited in the volume V probed by the laser is given

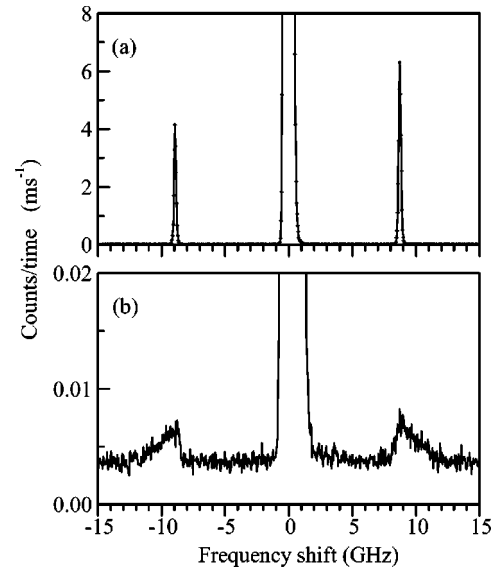


FIG. 2. BLS spectra (a) with 813 mW microwave pumping at 8.8 GHz and (b) without microwave pumping.

$$N_u = \frac{4V\omega_r}{\hbar} \left(\frac{h_m}{\Delta_H} \right)^2 \frac{\mu_0(H_r + M)M}{[\mu_0\gamma(2H_r + M)]^2}, \quad (3)$$

where H_r is the static field, M is the effective saturation magnetization, ω_r is the FMR angular frequency, Δ_H is the FMR field linewidth, h_m is the microwave magnetic field amplitude at the specimen, and γ is the gyromagnetic ratio of Permalloy, $1.84 \times 10^{11} \text{ T}^{-1} \text{ s}^{-1}$.

For our measurements, h_m is estimated to be 57 A/m with 1 W of absorbed microwave power. M is approximately 7.8×10^5 A/m, based on the measured H_r , ω_r , and the Kittel relation, $\omega_r = \mu_0\gamma[H_r(H_r + M)]^{1/2}$. Δ_H is determined to be $(3.9 \pm 0.4) \times 10^3$ A/m from the measured field dependence of BLS uniform-precession counts. V is approximately $3.6 \times 10^{-9} \text{ mm}^3$, assuming a diffraction-limited diameter of 17 μm for the laser spot and an effective thickness equal to the skin depth of 16 nm. Using these values and the slope of the line in Fig. 3, the cross section per magnon is estimated to be 1.2×10^{-2} counts/(s·W), where the units are of laser power and the time in a channel. Considering the assumption of a diffraction-limited spot size, this cross section should be considered to be an approximate upper limit.

Selective detection of magnons with nonzero wave vectors was accomplished by blocking the light scattered from uniform-precession magnons with an annular aperture having an inner diameter of 4 mm and an outer diameter of 21

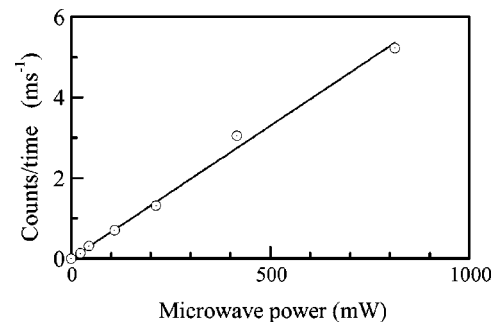


FIG. 3. Dependence of the count rate on the microwave power that is incident on the cavity.

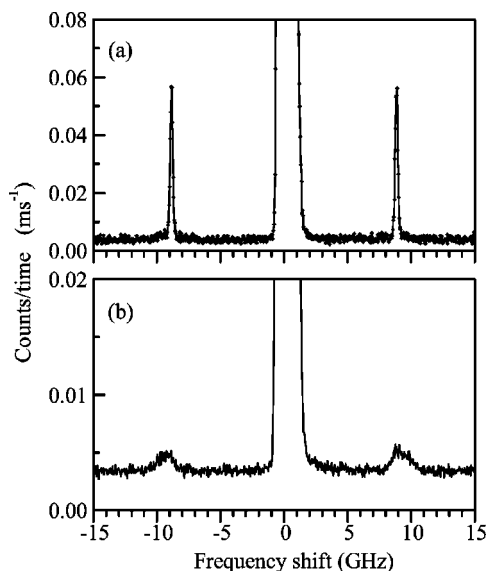


FIG. 4. BLS spectra with a 4 mm i.d. 21 mm o.d. annular aperture in the path of the backscattered light. (a) With 813 mW microwave pumping. (b) Without microwave pumping.

mm. The center of this annulus was centered on the specular reflection. From Eq. (2), the range of magnon wave vectors that can be detected in this configuration (with $d_1=3.3$ mm) is $4.7 \times 10^3 \text{ cm}^{-1}$ to $2.4 \times 10^4 \text{ cm}^{-1}$.

Figure 4 shows spectra with this aperture inserted. Microwave pumping greatly increases the counts at the pumping frequency as a result of scattering from magnons that are degenerate with the uniform precession. Such degenerate magnons can be generated in pumped ferromagnetic material through two-magnon processes.¹¹ In the absence of pumping [Fig. 4(b)], the spectrum arising from thermally excited mag-

nons is similar to that obtained without the aperture [Fig. 2(b)]. This indicates that most of the thermal magnons in the film have wave numbers greater than $4.7 \times 10^3 \text{ cm}^{-1}$.

In this letter, we have presented a method for performing backscattering BLS measurements on pumped uniform-precession and low- k magnons in opaque materials. Our demonstration of the method includes observation of pumped nonzero-wave-vector magnons in Permalloy [Fig. 4(a)]. This extension of the backscattering BLS technique will supply important complementary information to standard FMR and time-domain techniques and will help in achieving an understanding of magnetization dynamics under impulse excitation conditions.

We thank Professor John Cochran for suggesting the general approach that is presented here.

¹A. A. Serga, S. O. Demokritov, B. Hillebrands, and A. N. Slavin, *Phys. Rev. Lett.* **92**, 117203 (2004).

²A. N. Slavin, O. Bttner, M. Bauer, S. O. Demokritov, B. Hillebrands, M. P. Kostylev, B. A. Kalinikos, V. V. Grimalsky, and Yu. Rapoport, *Chaos* **13**, 693 (2003).

³T. J. Silva, C. S. Lee, T. M. Crawford, and C. T. Rogers, *J. Appl. Phys.* **85**, 7849 (1999).

⁴T. J. Silva, P. Kabos, and M. R. Pufall, *Appl. Phys. Lett.* **8**, 2205 (2002).

⁵T. J. Silva, M. R. Pufall, and P. Kabos, *J. Appl. Phys.* **91**, 1066 (2002).

⁶G. Srinivasan, C. E. Patton, and J. G. Booth, *J. Appl. Phys.* **63**, 3344 (1988).

⁷W. Wettleing and W. Jantz, *J. Magn. Magn. Mater.* **45**, 364 (1984).

⁸S. O. Demokritov, *J. Magn. Magn. Mater.* **126**, 291 (1993).

⁹J. R. Sandercock, in *Light Scattering in Solids III, Topics in Applied Physics Vol. 51*, edited by M. Cardona and G. Güntherodt (Springer, Berlin, 1982), pp. 173–206.

¹⁰V. L. Safonov, *J. Appl. Phys.* **91**, 8653 (2002).

¹¹M. Sparks, *Ferromagnetic Relaxation Theory* (McGraw-Hill, New York, 1964).